Innovative Food Science and Emerging Technologies 21 (2014) 179–187

Contents lists available at ScienceDirect

Innovative Food Science and Emerging Technologies

journal homepage: www.elsevier.com/locate/ifset

Non-destructive and rapid determination of TVB-N content for freshness evaluation of grass carp (*Ctenopharyngodon idella*) by hyperspectral imaging

Jun-Hu Cheng [a], Da-Wen Sun [a,b,*], Xin-An Zeng [a], Hong-Bin Pu [a]

[a] College of Light Industry and Food Sciences, South China University of Technology, Guangzhou 510641, China
[b] Food Refrigeration and Computerized Food Technology, Agriculture and Food Science Centre, University College Dublin, National University of Ireland, Belfield, Dublin 4, Ireland

A R T I C L E I N F O

Article history:
Received 2 September 2013
Accepted 26 October 2013

Editor Proof Receive Date 25 November 2013

Keywords:
Hyperspectral imaging
Non-destructive
TVB-N value
Successive projections algorithm
Wavelength selection
Grass carp

A B S T R A C T

Hyperspectral imaging technique in the spectral wavelength range of 400–1000 nm was implemented in this study to determine the total volatile basic nitrogen (TVB-N) contents of grass carp fillets during the frozen storage. The quantitative calibration models were built between the spectral data extracted from the hyperspectral images and the reference measured TVB-N values by using partial least squares regression (PLSR) and least squares support vector machines (LS-SVM). The LS-SVM model using full spectral range had a better performance than the PLSR model for prediction of TVB-N value with the corresponding coefficients of determination (R^2_P) of 0.916 and 0.905, and root-mean-square errors of prediction (RMSEP) of 2.346% and 2.749%, respectively. Nine optimal wavelengths (420, 466, 523, 552, 595, 615, 717, 850 and 955 nm) were selected using successive projections algorithm (SPA), and R^2_P values of 0.902 and 0.891 with the corresponding RMSEP of 2.782% and 2.807% were obtained from the new optimized models established based on the selected valuable wavelengths. The best SPA-LS-SVM model was used to achieve the visualization map of TVB-N content distribution of the tested fish fillet samples. The results of this study indicated that hyperspectral imaging technique as an objective and promising tool is capable of determining TVB-N values for evaluation of fish freshness quality in a rapid and non-destructive way.

Industrial relevance: The study showed that VIS–NIR hyperspectral imaging technique was an effective and powerful tool for rapid and non-destructive determination and assessment of fish fillet freshness for the fish industry.

1. Introduction

Along with the rapid development of fishery economy and continually increasing consumption of aquatic products such as fish as well as the improvement of healthy eating habits, consumers tend to put forward much higher requirements in fish quality control and assurance. However, the basic technological problem associated with such seafood is its vulnerability and perishability that has a strong impact on the freshness quality (Rzepka, Özogul, Surówka, & Michalczyk, 2013). In terms of fish freshness, it is nowadays stimulating great interest and attention to fishers, producers, retailers and consumers. Besides, it has always been acknowledged that freshness as one of the most important quality attributes is common in assessing the quality of fish, either for direct consumption or as raw materials for the processing industry (Gallart-Jornet, Rustad, Barat, Fito, & Escriche, 2007; Özogul, Özyurt, Özogul, Kuley, & Polat, 2005) and also it is the most focused property for the consumers because of its strong relationship with the taste quality (Alimelli et al., 2007; Quevedo, Aguilera, & Pedreschi, 2010). On the other hand, it has also been documented that freshness is difficult to be clearly defined and accurately measured due to diverse influencing factors (Poli, Parisi, Scappini, & Zampacavallo, 2005). In details, the freshness quality features to a large extent consist of a series of parameters related to safety, nutritional quality, availability, and edibility, which may be affected mainly by handling, processing and storage procedures from the catch to the consumers (Cheng, Sun, Zeng, & Liu, 2013; Norton & Sun, 2008). From another point of view, physical, chemical, biochemical and microbiological changes taking place in the postmortem of fish muscle result in a progressive loss of freshness characteristic and then influence the final eating quality of the products (Alimelli et al., 2007).

Therefore, besides the necessities to use novel methods such as rapid cooling (Sun & Brosnan, 1999; Sun & Zheng, 2006; Sun & Hu, 2003; Wang & Sun, 2001), drying (Cui, Xu, & Sun, 2004) and other techniques (Xu, Chen, & Sun, 2001) to preserve product quality, it is much more imperative to determine fish. On one hand, there are many well established traditional analytical techniques and methods available (Cheng et al., 2013; Dowlati et al., 2013), they mostly include sensory evaluation involving the use of sight, tactile and olfaction (Alimelli et al., 2007) and further developed quality index method (QIM) (Pons-Sanchez-Cascado, Vidal-

* Corresponding author. Tel.: +353 1 7167342; fax: +353 1 7167493.
E-mail address: www.dawen.sun@ucd.ie (D.-W. Sun).
URL's: http://www.ucd.ie/refrig.com, http://www.ucd.ie/sun.com (D.-W. Sun).

1466-8564/$ – see front matter © 2013 Elsevier Ltd. All rights reserved.
http://dx.doi.org/10.1016/j.ifset.2013.10.013

Carou, Nunes, & Veciana-Nogues, 2006), microbial inspection with the index of total viable counts (Song, Luo, You, Shen, & Hu, 2011), biochemical methods of determining ATP (adenosine triphosphate) degradation and calculating K value related to high-performance liquid chromatography (Mendes, Cardoso, & Pestana, 2009), chemical volatile compound measurement using solid-phase micro-extraction gas chromatography–mass spectrometry (Iglesias et al., 2009), protein property determination by two-dimensional difference gel electrophoresis (Addis et al., 2012) and proteome analysis (Carrera, Cañas, & Gallardo, 2012), and some other important spoilage/freshness indicators including total volatile basic nitrogen (TVB-N), trimethylamine (TMA) and formation of biogenic amine (Özogul et al., 2005). These techniques and methods play a pivotal role in the current research of fish freshness quality and safety evaluation and inspection and some of them have been used as excellent standards and supervision regulations with the purpose of maintaining freshness in the diverse distribution stages and providing consumers with high-quality products. These techniques and methods, however, need highly skilled operators, and are normally expensive, time-consuming, laborious, tedious, and not always available along the different procedures of the fishery chain and in particular not suitable for on/in-line monitoring. Consequently, in order to satisfy an increasing demand for on-site measurement of freshness quality ranging from capture to purchasing by consumers in the fish industry, non-destructive and rapid techniques and methods are in urgent need. Previous investigations have evidenced that some non-invasive and rapid measurement techniques have been developed for assessment of fish freshness during storage, including using computer vision (Dowlati, Guardia, & Mohtasebi, S. S., 2012; Mathiassen, Misimi, Bondø, Veliyulin, & Østvik, 2011; Zion, 2012) for fish quality grading (Misimi, Mathiassen, & Erikson, 2007), color and firmness measurement (Quevedo & Aguilera, 2010), and using molecular spectroscopy for fish freshness evaluation (Cozzolino & Murray, 2012; Nilsen, Esaiassen, Heia, & Sigernes, 2002) with its main features for prediction of chemical compositions, and using near infrared reflectance spectroscopy for origin identification of European sea bass (Xiccato, Trocino, Tulli, & Tibaldi, 2004), using visible spectroscopy for predicting sensory scores of cod (Nilsen & Esaiassen, 2005), as well as using front-face fluorescence spectroscopy (Dufour, Frencia, & Kane, 2003) and mid-infrared spectroscopy (Karoui et al., 2007) for monitoring fish freshness. However, using computer vision (Du & Sun, 2005) alone, it cannot provide chemical composition information of the products, on the other hand, only spectroscopic techniques cannot directly offer the spatial distribution and visualization information. To overcome these difficulties, an imaging technique is necessary to map the position of each spatially resolved component. As an innovative platform technology, hyperspectral imaging technique has been emerged to conquer the shortcomings of spectroscopy and computer vision mentioned above by means of integrating the techniques of spectroscopy and imaging into one system. Generally speaking, a typical spectrometer offers a single spectrum, $I(\lambda)$, while imaging provides the intensity at each pixel of the image, $I(x, y)$. Thus, a spectral image provides a spectrum at each pixel $I(x, y, \lambda)$, which can be viewed as a cube of information (Zhang, Liu, He, & Li, 2012). Therefore, this emerging technique can create a three-dimensional (3D) dataset that contains many images of the same object, and each of which is measured at a different wavelength. Owing to the abilities of space distinguishing and spectral resolution, spectral imaging can obtain both the spatial and spectral information of the object simultaneously (Sun, 2010). Fig. 1 shows the schematic illustration of the hyperspectral image cube.

Recently, the aptitude of hyperspectral imaging technique has been widely developed in food quality and safety evaluation and inspection (Elmasry, Kamruzzaman, Sun, & Allen, 2012; ElMasry, Sun, & Allen, 2012; Feng & Sun, 2012). A number of studies have highlighted the performance of hyperspectral imaging technique coupled with appropriate chemometric multivariate analysis and it has been proved that the technique possesses a great potential for simultaneous assessment of various chemical constituents without using hazardous chemical reagents and was successfully applied for categorization and authentication of red meat (pork, beef, lamb) (Kamruzzaman, Barbin, ElMasry, Sun, & Allen, 2012; Kamruzzaman, ElMasry, Sun, & Allen, 2012), assessment and mapping of beef quality related to water, fat, protein content (ElMasry, Sun, & Allen, 2013), tenderness and color parameters (Elmasry, Kamruzzaman et al., 2012; ElMasry, Sun et al, 2012) and water-holding capacity (ElMasry, Sun, & Allen, 2011); detection of poultry surface fecal contaminant (Park, Lawrence, Windham, & Smith, 2006) and determination of *Enterobacteriaceae* on chicken fillets (Feng & Sun, 2012); prediction and visualization of lamb involving chemical compositions and pH, color and drip loss (Kamruzzaman, Barbin et al, 2012, Kamruzzaman, ElMasry et al. 2012); study of growth characteristics and differences between species and strains of members of the genus *Fusarium* (Williams, Geladi, Britz, & Manley, 2012a, 2012b); determination of TVC, *Enterobacteriaceae* and *Pseudomonas* loads in chicken breast fillets (Feng & Sun, 2013); assessment of microbial contamination in porcine meat (Barbin, ElMasry, Sun, Allen, & Morsy, 2012); prediction of moisture, color, pH and protein contents and quality classification of cooked hams (Talens et al., 2013); grading and classification of pork (Barbin, Elmasry, Sun and Allen, 2012a, 2012b); prediction of sensory attributes (Barbin, Elmasry, Sun and Allen, 2012a, 2012b), chemical compositions (Barbin, Elmasry, Sun and Allen, 2012a, 2012b), and recognition of fresh and frozen–thawed pork muscles (Talens et al., 2013). In addition, this technique has also been studied for evaluation of fish and fish product quality with high performance for classifying fresh Atlantic salmon fillets (Sone, Olsen, Sivertsen, Eilertsen, & Heia, 2012) and sea bass cultured under different

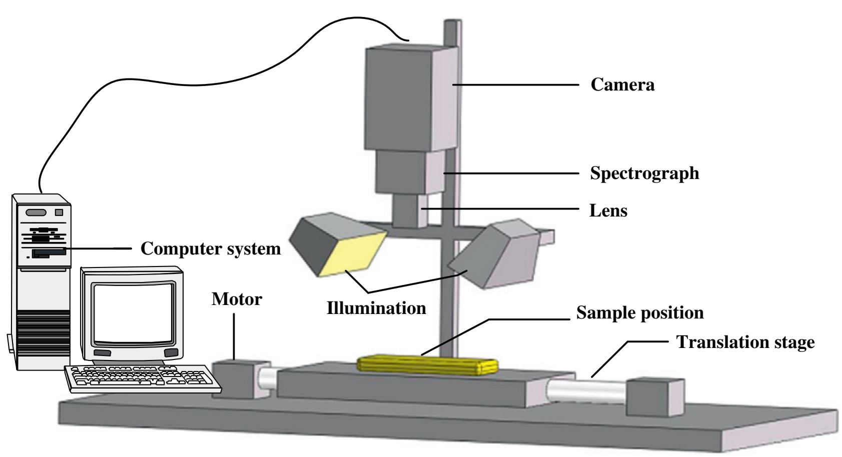

Fig. 1. Schematic diagram of main components of VIS–NIR hyperspectral imaging system.

conditions (Costa et al., 2011), determination of microbial spoilage of salmon flesh (Wu & Sun, 2013), detection of expired vacuum-packed smoked salmon (Ivorra et al., 2013), analysis of moisture distribution in farmed Atlantic salmon fillets (He, Wu, & Sun, 2013), measurement of color features in salmon fillets (Wu, Peng, Li, Wang, Chen and Dhakal, 2012, Wu, Shi, Wang, He, Bao and Liu, 2012, Wu, Sun and He, 2012) and gilthead sea bream (Costa et al., 2012), evaluation of fish freshness (Menesatti, Costa, & Aguzzi, 2010), and detection of nematode in cod fillets (Sivertsen, Heia, Hindberg, & Godtliebsen, 2012; Sivertsen, Heia, Stormo, Elvevoll, & Nilsen, 2011).

Despite the above investigations, there is no study reported yet about the determination of TVB-N index for evaluation of fish freshness using visible and near infrared (VIS–NIR) hyperspectral imaging. Therefore, in this study, VIS–NIR hyperspectral imaging technique was applied to evaluate its potential for measurement and prediction of TVB-N value of grass carp (*Ctenopharyngodon idella*). The overall objective of this study aimed to investigate whether freshness of fish could be successfully assessed by VIS–NIR hyperspectral imaging.

2. Materials and methods

2.1. Preparation of fish fillet samples

Thirty fresh grass carps each approximately weighting 1.5 kg were purchased from a local aquatic products market of Sushi in Guangzhou, China, and immediately transported to the laboratory alive. The fresh grass carps were slaughtered, beheaded, gutted, skinned, and filleted and then washed with cold water. One hundred and twenty fillets with similar size were obtained and packaged in plastic film for freezing storage. All fillets were frozen at −20 °C for 24 h using a cryogenic refrigerator, these frozen samples were then thawed at 4 °C for 12 h, which was defined as one freezing–thawing cycle in the current study for convenience. Thawed samples were again frozen for 24 h, followed by thawing for different cycles, with the purpose of simulating temperature abuse in supply chains. Samples without freezing–thawing were referred to as "zero freezing–thawing cycle" and the fish fillets in this condition were fresh and of superior quality. Thus, the fillet samples were subjected to zero, one, two, and three freezing–thawing cycles, respectively. And each time the randomly selected thirty fillet samples were placed on ice for further analysis.

2.2. Determination of TVB-N

TVB-N value was determined by a stream distillation method with some modifications (Cai, Chen, Wan, & Zhao, 2011). Ten grams of grass carp muscle was minced and then mixed with 90 mL of perchloric acid (0.6 M) and centrifuged at 3000 rpm for 10 min, and the filtrate was made alkaline by adding 50 mL of 30% sodium hydroxide and distilled for 5 min in a 8100 Kjeltec Distillation Unit (FOSS Tecator, Denmark), and 50 mL of distilled water was used as control. The distillate was collected in a conical flask containing 50 mL aqueous solution of boric acid (40 g/L) and a mixed indicator created from dissolution of 0.1 g of methyl red and 0.1 g of bromocresol green into 100 mL of 95% ethanol. Afterward, the obtained boric acid solution was titrated with a 0.01 M of hydrochloric acid solution. The TVB-N value was measured and expressed as mg N/100 g fish muscle according to the consumption of hydrochloric acid. Each analysis was repeated in triplicate.

2.3. Hyperspectral imaging system

A hyperspectral imaging system with common pushbroom configuration was applied to obtain the hyperspectral images of grass carp fillets in reflectance mode. This system mainly consisted of a line-scan imaging spectrograph (Imspector V10E, Spectral Imaging Ltd., Oulu, Finland) covering the spectral range of 308–1105 nm, a high performance CCD camera (DL-604 M, Andor, Ireland) with the effective resolution of 1004 × 1002 pixels, a camera lens (OLE23, Schneider, German), a light source system including two 150 W halogen lamps (2900-ER, Illumination Technologies Inc., New York, USA) equipped with a fiber optical line light located at an angle of 45° to illuminate the moving platform operated by a stepping motor (IRCP0076-1COMB, Isuzu Optics Corp., Taiwan, China), a computer with imaging data acquisition software (Spectral Image software, Isuzu Optics Corp., Taiwan, China), which shows and regulates the exposure time, motor speed, combining mode, wavelength range and image acquisition. In this study, the working spectral range of this system was 308–1105 nm with a spectral increment of about 1.5 nm between the contiguous bands, thus producing a total of 501 bands. The spectral range of 400–1000 nm was considered and used for analyses due to low signal-to-noise out of this spectral range. Fig. 1 illustrates the schematic diagram of main components of the VIS–NIR hyperspectral imaging system.

2.4. Image acquisition and calibration

For each freezing–thawing cycle, thirty grass carp fillets were placed on the moving platform and then transferred to the field of the vision of the camera to be scanned line by line with the adjusted speed of 1.5 mm/s to coordinate with the image acquisition. Thus, a total of 120 hyperspectral images were produced, recorded and stored in a raw format before being processed. Two thirds of the fillet samples (80 fillets) were used as the calibration set and the rest of 40 samples were regard as the prediction set. The relevant statistics information of TVB-N value is illustrated in Table 1.

In order to minimize the effects of illumination and detector sensitivity as well as the differences in camera and physical configuration of the imaging system, the original acquired hyperspectral images (R_0) were necessary to be calibrated into the reflectance mode with two extra images for black (B) and standard white (W) reference images. The black image (~0% reflectance) was obtained by noting a spectral image after fully covering the camera lens with its black cap. The white reference image was acquired using a uniform Teflon white tile (~99% reflectance). The calibrated image (R_C) was calculated by the following formula.

$$R_C = \frac{R_0 - B}{W - B} \times 100\%. \tag{1}$$

2.5. ROI identification and spectra extraction

After image acquisition and reflectance calibration, the region of interests (ROIs) with an ellipse shape within hyperspectral images were recognized and selected based upon the important locations corresponding to areas of the ten grams of grass carp fillets that were used in the reference measurements. Then the extracted, averaged and recorded spectral data within ROIs for the samples were conducted by using the software ENVI v4.8 (ITT Visual Information Solutions, Boulder, CO, USA).

Table 1
Reference values of TVB-N content (mg N/100 g) measured by a traditional method.

Statistics	Calibration	Prediction
Minimum	7.83	8.02
Maximum	16.48	15.85
Mean	12.22	11.94
Standard deviation	5.28	5.13
Range	8.65	7.83

2.6. Multivariable data analysis

The enormous spectral data extracted from hyperspectral images contain a significant amount of useful information and certainly there is some redundant information affecting the calibration. In order to improve the predictive ability and reduce the variability between samples due to scatter and optical interference possibly caused by water movement in frozen storage, multiplicative scatter correction (MSC) as a widely used spectral pre-processing technique was applied to eliminate the undesirable scatter effect from the data matrix prior to data modeling (Maleki, Mouazen, Ramon, & De Baerdemaeker, 2007; Rinnan, Berg, & Engelsen, 2009; Zeaiter, Roger, & Bellon-Maurel, 2005). After spectral pre-processing, it is necessary to select a robust and reliable analytical method to process and build a calibration model for quantitative or qualitative analysis. In this study, the quantitative calibration models between the spectral data and the TVB-N values were established by partial least squares regression (PLSR) and least squares support vector machines (LS-SVM), which was a typical linear and a classical nonlinear modeling method, respectively. It is well-known that PLSR, as one of the important and highly effective multivariate data analysis methods, has been widely developed for establishment of mathematical model due to its better flexibility in some conditions such as variable number more than sample number and multicollinearity among X values (Abdi, 2010). Support vector machines (SVM) have been very successful in pattern recognition and function estimation problems (Suykens, Vandewalle, & De Moor, 2001) and LS-SVM is an alternate and developed formulation of SVM, which involves equality instead of inequality constraints and works with a least squares cost function. LS-SVM has been introduced for the optimal control of nonlinear systems (Chauchard, Cogdill, Roussel, Roger, & Bellon-Maurel, 2004; Nicolaï, Theron, & Lammertyn, 2007; Suykens, De Brabanter, Lukas, & Vandewalle, 2002). This methodology utilizes nonlinear map function and map features into a high dimensional space and adopts the Lagrange multiplier to compute the partial differentiation of each feature to achieve the optical resolution (Cawley & Talbot, 2002; Suykens et al., 2001). The execution step of this algorithm was described in details by Chauchard et al. (2004) and Suykens et al. (2001). The performances of the two established models based upon PLSR and LS-SVM using the full spectral range were compared and evaluated according to their capability of prediction. The predictive effectiveness, reliability and accuracy of the established models were commonly assessed in terms of coefficients of determination and root mean square errors in calibration, leave-one-out cross-validation and prediction, respectively (R^2_C, R^2_{CV}, and R^2_P; RMSEC, RMSECV and RMSEP). Most importantly, it has been proved that an admirable and comparable prediction model should have higher values of R^2_C, R^2_{CV}, and R^2_P, and lower values of RMSEC, RMSECV and RMSEP as well as a small difference between them. In this study, LS-SVM was carried out using Matlab 2010a software (The MathWorks Inc., Mass, USA).

2.7. Optimal wavelength selection

Hyperspectral images of each fish fillet sample obtained by using this hyperspectral imaging system within the working spectral range of 400–1000 nm in this study were characterized as high dimensionality with redundancy and multicollinearity among contiguous wavelength bands, which to some extent resulted in the consequent time-consuming calibration process and affected the speed of computation related to the processing of the hyperspectral images. Thus, it is a critical procedure to reject the useless or unnecessary wavelengths with irrelevant information and select optimal wavelengths carrying the most valuable information that reflected the changes of TVB-N during multivariate analysis. However, selecting the optimal wavelengths (variables) from the whole spectral wavelength range is of difficulty due to the fact that there is no universal variable selection method for wide applications yet. Successive projections algorithm (SPA), as a forward variable selection method, has been proved to be a useful and effective tool and strategy for variable selection in the framework of multivariate calibration with the aim of resolving the problem of colinearity with minimal redundancy (Moreira, Pontes, Galvão, & Araújo, 2009; Pontes et al., 2005; Xiaobo, Jiewen, Povey, Holmes, & Hanpin, 2010). This popular algorithm usually begins with one variable/wavelength, and then incorporates a new one at each iteration, until a specified number N of variables/wavelengths is reached (Ghasemi-Varnamkhasti et al., 2012). The description and detailed implementation steps of this algorithm was reported in the study of Araújo et al. (2001). In the current study, SPA was used to choose the most important and sensitive wavelengths, carrying the most abundant and valuable freshness quality information, which contributed to predicting TVB-N values for evaluation of fish freshness quality. The procedure of SPA was conducted in Matlab 2010a software (The MathWorks Inc., Mass, USA).

2.8. Visualization of chemical image

The total volatile basic nitrogen mainly involves the ammonia and amines resulting from the degradation of proteins caused by the effects of enzymes and microorganisms activities and the content of this important index can effectively reflect the loss of freshness quality. Therefore, visualization of TVB-N distribution is helpful to further interpret the dynamical changes of the chemical compounds related to protein decomposition for indication of the degree of freshness loss. Hyperspectral imaging technique as a useful chemical imaging tool is capable of visualizing the spatial distribution of chemical components by generating the images or maps of concentration gradients. In this study, the new selected optimized calibration model was used to transfer and visualize every pixel of the hyperspectral images into the chemical images for prediction of TVB-N distribution of the examined fish fillets. The received chemical images or visualized distribution map was exhibited in a linear color scale with different colors, representing corresponding concentration of the predicted TVB-N in the whole grass carp fillet, which is advantageous to adjudicate and understand the variations of TVB-N content by checking the different color distribution. All the procedures of visualization were achieved by a computer program operated in the software Matlab 2010a (The MathWorks Inc., Mass, USA). Fig. 2 describes the whole procedure of the experiment by using hyperspectral imaging technique.

3. Results and discussion

3.1. Spectral characteristics of the fresh and treated fish fillet

Fig. 3 shows the average reflectance spectra extracted from the grass carp fillets in hyperspectral images within the wavelength region of 400–1000 nm. In Fig. 3, it was obviously identified that a similar tendency was displayed throughout the examined wavelength region at different TVB-N values with the range of 7–17 mg N/100 g, but there were some differences in the amplitude of variation of spectral reflectance. This was possibly attributed to the changes of the main chemical components during the freshness loss of grass carp fillet. According to the value of reflectance, a conspicuous and significant absorption peak was positioned at just about 500 nm, possibly associated with the residue of organic feed ingredients such as soybean meal, which was different from the reason of the absorption of carotenoids such as astaxanthin and canthaxanthin in salmon fillet muscle (Kimiya, Sivertsen, & Heia, 2013). Another absorption peak located at about 780 nm in the NIR region was mainly due to the third overtone O – H stretching (He et al., 2013). Absorption by water was observed as a peak close to 970 nm was largely ascribed to the second overtone O – H stretching (Wu & Sun, 2013; Zhu et al., 2012). Another interesting peak centered nearly at 430 nm was observed and there were few reports about this specific wavelength in grass carp except the reason of absorption by heme-pigment such as hemoglobin in cod fillets

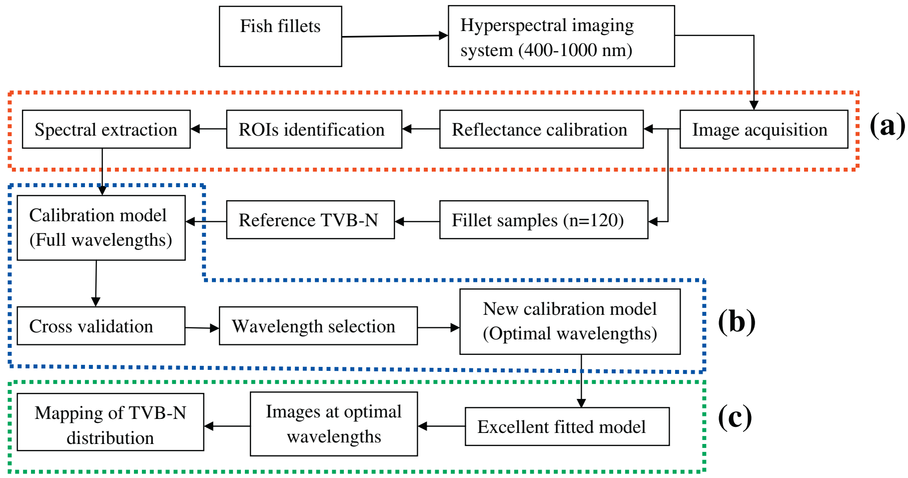

Fig. 2. Main steps of determination of TVB-N content in grass carp fillet using hyperspectral imaging. (a) Imaging pre-processing; (b) Spectral analysis; (c) Imaging post-processing.

(Sivertsen et al., 2012). With respect to the possible reasons, it would be associated with the wavelength calibration error or the alignment of the instruments.

3.2. Prediction of TVB-N values based on the whole spectral wavelength range

Throughout all the spectral dataset extracted from the hyperspectral images of grass carp fillets and their relevant reference measured TVB-N values, the prediction models were conducted and established based upon PLSR and LS-SVM algorithms using the whole spectral wavelengths within the range of 400–1000 nm, respectively. With respect to the predicted and measured values of TVB-N of fish fillet samples, their corresponding quantitative relationship was also obtained and shown in Table 2 and Fig. 4. It is clear that selecting a best calibration model is of significance in spectral analysis and of great contributions to the subsequent prediction. Therefore, in this study, the better fitted calibration method was chosen by comparing the performances of the two typical calibration methods. It can be seen from Table 2, when PLSR was used to build the calibration model, the values of the three coefficients of determination (R^2_C, R^2_{CV}, R^2_P) were 0.927, 0.913, and 0.905, respectively with the corresponding root mean square error (RMSEC, RMSECV, and RMSEP) of 2.258, 2.634, and 2.749, accompanying with a fairly small absolute deviation of 0.376, 0.491, and 0.115 between them. The values obtained above displayed a better performance than that of another study reported by He et al. (2013) for rapid analysis of moisture distribution in farmed Atlantic salmon fillets using VIS–NIR hyperspectral imaging, showing the values of 0.911, 0.897, and 0.893 using the same modeling approach. Additionally, in comparison with the resultant PLSR model, a relatively better value was obtained by using LS-SVM algorithm to establish the calibration model, in spite of a minor increase of 0.007, 0.008, and 0.011 for R^2_C, R^2_{CV} and R^2_P, but a decrease of 0.271, 0.399, and 0.403 for RMSEC, RMSECV and RMSEP. Therefore, according to the basic standard and requirement for evaluating the calibration models, it was confirmed that the model established by LS-SVM approach using full spectral range had a better performance than that by PLSR for prediction of TVB-N value of grass carp fillets. Another work reported by Wu, Peng (2012),Wu, Shi (2012), and Wu, Sun (2012) who have also been convinced by the same results and indicated that this modeling method was better and more effective for rapid prediction of moisture content of dehydrated prawns using hyperspectral imaging system. More importantly, the capability of predictive model was proved to be accurate and robust by the acquired model and the valuable data, and this hyperspectral imaging technique had the potential to have the ability of determining TVB-N values of fish fillets in a non-destructive manner.

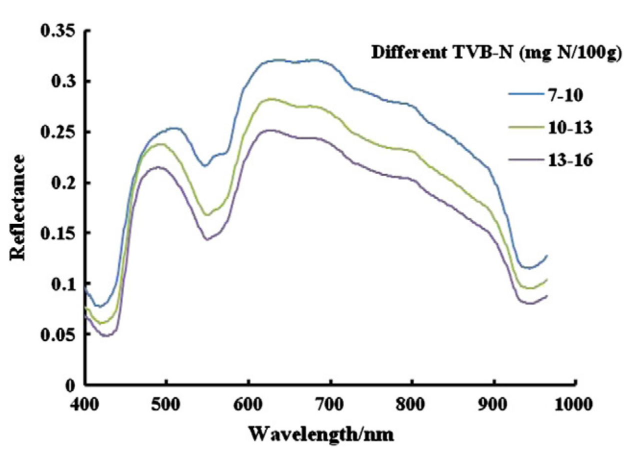

Fig. 3. Average spectral features of the tested grass carp fillets at different TVB-N values.

3.3. Prediction of TVB-N values based on only optimal wavelengths

In order to minimize the inessential and redundant information obtained from the hyperspectral images and optimize and redesign the structure of imaging detection system, it is obviously significant to select the optimal wavelengths. SPA has been widely developed and considered as one of the most effective methods in variable selection. Therefore, in this study, this algorithm was conducted to choose the most important wavelength variables carrying the most abundant and valuable information related to the fish freshness quality from the whole spectral range. As the result, nine wavelength variables (420, 466, 523, 552, 595, 615, 717, 850 and 955 nm) were elected as the optimal wavelengths, which were then used for subsequent prediction of the TVB-N values of fish fillets. These selected wavelengths almost covered the whole spectral range and possessed the advantages of minimal redundancy with the most sensitive information. Meanwhile, they were mainly located upon the region of visible spectrum, such as 420 nm, 466 nm, 523 nm, 552 nm, 595 nm, 615 nm and 717 nm. However, few reports were available to explain this phenomenon. The possible reasons were allied to the variations of color and texture during the freezing and thawing process. The selected important wavelength located at 955 nm was ascribed to the water absorption band due to the fact that water is the major component in the fish muscle. Another peak at 850 nm was usually assigned to the stretching overtones of C – H, and N – H that was associated with protein, lipid and other organic compositions (Howard & Kjaergaard, 2006; Tarr & Zerbetto, 1989). Similar to the modeling method based on the full spectral wavelength range, the

Table 2
Calibration and prediction results of the TVB-N value of grass carp fillet by hyperspectral imaging technique.

Calibration model	Variable number	No. of latent variable	Calibration		Cross-validation		Prediction	
			R^2_C	RMSEC (%)	R^2_{CV}	RMSECV (%)	R^2_P	RMSEP (%)
PLSR	378	8	0.927	2.258	0.913	2.634	0.905	2.749
LS-SVM	378	/	0.934	1.987	0.921	2.235	0.916	2.346
SPA-PLSR	9	6	0.910	2.718	0.899	2.786	0.891	2.807
SPA-LS-SVM	9	/	0.918	2.246	0.912	2.401	0.902	2.782

optimized PLSR and LS-SVM, also referred to as SPA-PLSR and SPA-LS-SVM, were implemented to establish the innovative models for prediction of freshness quality of grass carp fillets based upon the spectral information of nine optimal wavelengths and the statistical results are illustrated in Table 2. The values of R^2_C, R^2_{CV} and R^2_P were 0.910, 0.899 and 0.891, and 0.918, 0.912 and 0.902 based on the developed SPA-PLSR and SPA-LS-SVM models, respectively. The corresponding absolute deviations of root mean square error (RMSEC, RMSECV and RMSEP) are shown to be 0.068, 0.0.089 and 0.021, and 0.155, 0.536 and 0.382, respectively, which were better than the results reported by Cai et al. (2011), who revealed that the values of R^2_C, and R^2_P were 0.840 and 0.808 for TVB-N content of pork meat using synergy interval PLSR algorithm by Fourier transform near infrared spectroscopy. In addition, it was easy to discover that from the resultant data, there were minor differences among them, and the new simplified models using the optimal wavelengths were comparable to the original models using the whole wavelengths. Furthermore, it was also noticed that the SPA-PLSR model had poorer performance than the SPA-LS-SVM model that showed better accuracy and robustness with higher coefficient of determination and smaller root mean square error. Therefore, it could be seen from the above study that the novel developed models using optimal wavelengths exhibited equivalent predictive effectiveness and accuracy to the corresponding original models. Meanwhile, the optimized LS-SVM was more powerful in predicting TVB-N values than the simplified PLSR, which also demonstrated that SPA algorithm was suitable and competent for selecting the informative variables in this study. Therefore, SPA-LS-SVM was regarded as the best model using the optimal wavelengths replacing the full wavelengths to predict the TVB-N values for evaluation of freshness quality of the fresh and frozen fish fillets.

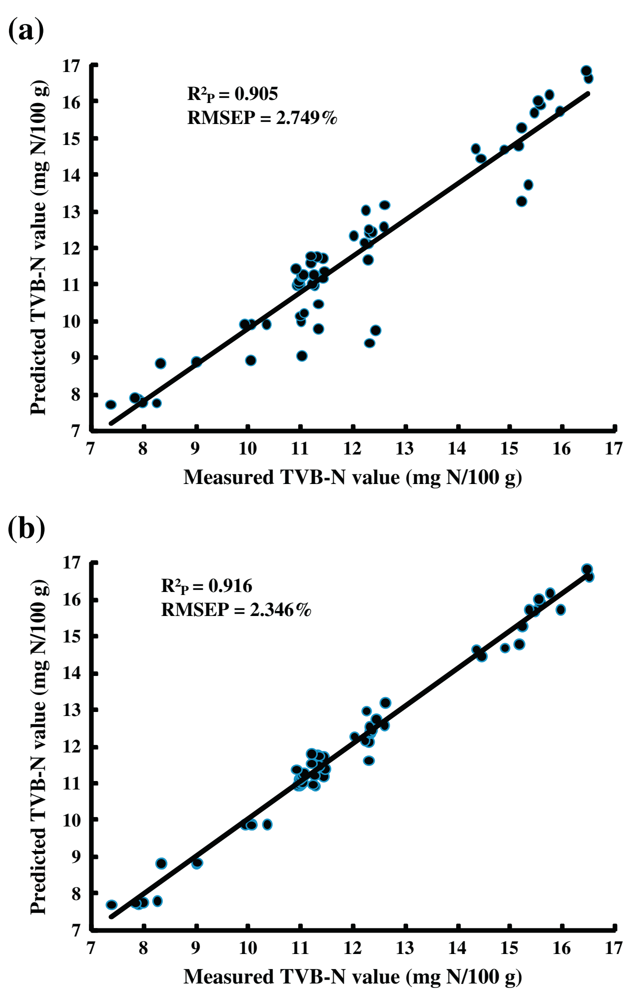

Fig. 4. Predicted and measured TVB-N values for both the PLSR (a) and LS-SVM (b) models under the whole spectral wavelengths range.

3.4. Visualization of TVB-N distribution of fish fillet sample

In fact, the limits of the freshness of various fish species are implemented with no unified standard based on TVB-N content in different countries and regions. For example, according to Chinese standard GB 2733, 2733 (2005), for marine fish, the rejection limit of TVB-N content is regarded as 30 mg N/100 g; for freshwater fish, the TVB-N content cannot exceed 20 mg N/100 g. Therefore, in order to better interpret the variations of TVB-N in different locations of fish fillets during frozen storage and control the quality of fish products, visualization of TVB-N distribution is obviously helpful and meaningful using a linear color bar to exhibit different colors from blue (low value) to red (high value) due to the fact that the pixels with similar spectral features in the distribution map created a similar visualized color for matching and representing the values of TVB-N. Therefore, in this study, the best developed model based on SPA-LS-SVM using the optimal wavelengths was considered as the most suitable model for TVB-N measurement due to its reliability and efficiency, and was also used to transfer each pixel of the hyperspectral image to its corresponding TVB-N value for visualization of TVB-N distribution in all spots of the grass carp fillets. Fig. 5 shows examples of visualization of TVB-N distribution map of fish fillet at three different TVB-N values. It was visibly observed that different colors in the visualized map reflected TVB-N contents in the fish fillet sample corresponding to the spectral changes of image pixels. It was also noticed that the density and intensity of TVB-N distribution of the grass carp fillet sample were non-uniform and asymmetric due to the fact that the total volatile basic nitrogen included all the compositions of degradation of nitrogen-containing chemical compounds such as proteins of fish muscle. Thus, the homogeneousness of TVB-N distribution was contributed to the speed of degradation of these chemical compounds. Some other possible reasons were mainly related to fish species, farming situations, feeding ingredients, and handling methods such as high-pressure processing, freezing–thawing, chilling, cold storage temperature and time (Cheng et al., 2013). In particular, the distribution of TVB-N content illustrated in Fig. 5a (TVB-N = 8.26 mg N/100 g) and Fig. 5b (TVB-N = 12.98 mg N/100 g) was fairly non-uniform along with different locations of fish fillet samples. It was clearly identified that the surrounding locations posed higher value than that of inner locations attributing to the reasonable fact that the external parts were subjected to the effects of activities of microorganisms and occurrence of autolysis. For example, in Fig. 5a, there is great extent of

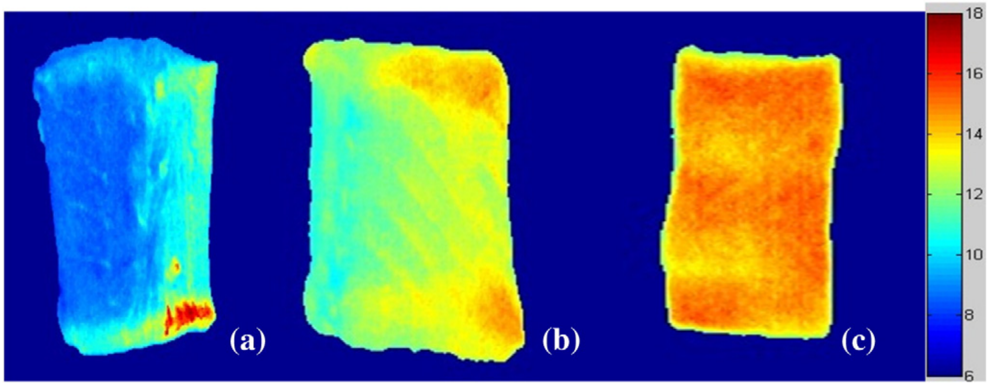

Fig. 5. Examples of visualization of TVB-N distribution map of fish fillet at three different TVB-N values. (a), (b) and (c) represent the TVB-N value of 8.26, 12.98, and 15.69 mg N/100 g, respectively.

low value of TVB-N in blue color, except some small regions showing red color that indicated high value of TVB-N. However, Fig. 5c (TVB-N = 15.69 mg N/100 g) shows moderately homogenous distribution of TVB-N content in the same red color, implying that a great level of degradation of chemical compounds occurred and consequently caused severe loss of freshness quality of fish fillets. Thus, it was appropriate to make certain the transformation process of TVB-N in the fish fillet during frozen storage by contrasting different distribution maps of TVB-N contents. Also, it was helpful and meaningful for further interpreting the dynamic changes of freshness quality that directly determined the acceptance of consumers. Most importantly, the results confirmed that a great advantage of hyperspectral imaging technique is to provide spatial information of the examined samples and to create the TVB-N distribution maps for evaluating the fish quality of freshness, in order to enhance fish quality control and ensure fish products safety. Additionally, it can be further inferred that this potential and innovative technique is capable of sorting and discriminating the fresh and frozen samples in the fish industry and evaluating the non-uniform distribution of fish samples due to the effects of different handling processes.

4. Conclusions

VIS–NIR hyperspectral imaging technique (400–1100 nm) in tandem with PLSR and LS-SVM was conducted to determine the TVB-N values of grass carp fillets for evaluation of fish freshness quality. The prediction models were established based upon PLSR and LS-SVM using the whole spectral wavelengths with high prediction ability with strong correlations (R^2_P = 0.905, 0.916). In addition, it was further shown that SPA was a useful variable selection method suitable for choosing nine optimal wavelengths (420, 466, 523, 552, 595, 615, 717, 850 and 955 nm) for prediction of TVB-N values. The developed SPA-LS-SVM calibration model using the nine selected wavelengths was superior and advantageous than the simplified SPA-PLSR model with the R^2_P value of 0.902 and 0.891, respectively, which was equivalent to the original models using the whole spectral wavelengths ranges. Additionally, visualization maps of TVB-N distribution were created using pseudo color for further understanding the loss of fish freshness during frozen storage. The current results showed that this VIS–NIR hyperspectral imaging technique was an effective and powerful tool for rapid and non-destructive determination and assessment of fish fillet freshness.

Acknowledgments

The authors were grateful to the Guangdong Province Government (China) for its support through the program of “Leading Talent of Guangdong Province (Da-Wen Sun)”. This research was also supported by the Foundation for the Author of National Excellent Doctoral Dissertation of South China University of Technology.

References

Abdi, H. (2010). Partial least squares regression and projection on latent structure regression (PLS Regression). *Wiley Interdisciplinary Reviews: Computational Statistics*, *2*(1), 97–106.

Addis, M. F., Pisanu, S., Preziosa, E., Bernardini, G., Pagnozzi, D., Roggio, T., et al. (2012). 2D-DIGE/MS to investigate the impact of slaughtering techniques on postmortem integrity of fish filet proteins. *Journal of Proteomics*, *75*(12), 3654–3664.

Alimelli, A., Pennazza, G., Santonico, M., Paolesse, R., Filippini, D., D'Amico, A., et al. (2007). Fish freshness detection by a computer screen photoassisted based gas sensor array. *Analytica Chimica Acta*, *582*(2), 320–328.

Araújo, M. C. U., Saldanha, T. C. B., Galvão, R. K. H., Yoneyama, T., Chame, H. C., & Visani, V. (2001). The successive projections algorithm for variable selection in spectroscopic multicomponent analysis. *Chemometrics and Intelligent Laboratory Systems*, *57*(2), 65–73.

Barbin, D., Elmasry, G., Sun, D. -W., & Allen, P. (2012a). Near-infrared hyperspectral imaging for grading and classification of pork. *Meat Science*, *90*(1), 259–268.

Barbin, D. F., ElMasry, G., Sun, D. -W., & Allen, P. (2012b). Non-destructive determination of chemical composition in intact and minced pork using near-infrared hyperspectral imaging. *Food Chemistry*, *138*(2–3), 1162–1171.

Barbin, D. F., ElMasry, G., Sun, D. -W., Allen, P., & Morsy, N. (2012). Non-destructive assessment of microbial contamination in porcine meat using NIR hyperspectral imaging. *Innovative Food Science & Emerging Technologies*, *17*, 180–191.

Cai, J., Chen, Q., Wan, X., & Zhao, J. (2011). Determination of total volatile basic nitrogen (TVB-N) content and Warner–Bratzler shear force (WBSF) in pork using Fourier transform near infrared (FT-NIR) spectroscopy. *Food Chemistry*, *126*(3), 1354–1360.

Carrera, M., Cañas, B., & Gallardo, J. M. (2012). Proteomics for the assessment of quality and safety of fishery products. *Food Research International*, http://dx.doi.org/10.1016/j.foodres.2012.10.027 (In press).

Cawley, G. C., & Talbot, N. L. (2002). Improved sparse least-squares support vector machines. *Neurocomputing*, *48*(1), 1025–1031.

Chauchard, F., Cogdill, R., Roussel, S., Roger, J., & Bellon-Maurel, V. (2004). Application of LS-SVM to non-linear phenomena in NIR spectroscopy: development of a robust and portable sensor for acidity prediction in grapes. *Chemometrics and Intelligent Laboratory Systems*, *71*(2), 141–150.

Cheng, J., Sun, D. -W., Zeng, X. -A., & Liu, D. (2013). Recent advances in methods and techniques for freshness quality determination and evaluation of fish and fish fillets: A review. *Critical Reviews in Food Science and Nutrition (accepted)*, http://dx.doi.org/10.1080/10408398.2013.769934.

Chinese standard GB 2733 (2005). *Hygienic standard for fresh and frozen marine products of animal origin.*

Costa, C., Antonucci, F., Menesatti, P., Pallottino, F., Boglione, C., & Cataudella, S. (2012). An advanced colour calibration method for fish freshness assessment: A comparison between standard and passive refrigeration modalities. *Food and Bioprocess Technology*, *1–6*.

Costa, C., D'Andrea, S., Russo, R., Antonucci, F., Pallottino, F., & Menesatti, P. (2011). Application of non-invasive techniques to differentiate sea bass (*Dicentrarchus labrax*, L. 1758) quality cultured under different conditions. *Aquaculture International*, *19*(4), 765–778.

Cozzolino, D., & Murray, I. (2012). A review on the application of infrared technologies to determine and monitor composition and other quality characteristics in raw fish, fish products, and seafood. *Applied Spectroscopy Reviews*, *47*(3), 207–218.

Cui, Z. W., Xu, S. Y., & Sun, D. -W. (2004). Effect of microwave-vacuum drying on the carotenoids retention of carrot slices and chlorophyll retention of chinese chive leaves. *Drying Technology*, *22*(3), 563–575, http://dx.doi.org/10.1081/DRT-120030001.

Dowlati, M., Guardia, M., & Mohtasebi, S. S., d. l. (2012). Application of machine-vision techniques to fish-quality assessment. *TrAC Trends in Analytical Chemistry*, *40*, 168–179.

Dowlati, M., Mohtasebi, S. S., Omid, M., Razavi, S. H., Jamzad, M., Guardia, M., et al. (2013). Freshness assessment of gilthead sea bream (*Sparus aurata*) by machine vision based on gill and eye color changes. *Journal of Food Engineering*, *119*(2), 277–287.

Du, C. J., & Sun, D. -W. (2005). Comparison of three methods for classification of pizza topping using different colour space transformations. *Journal of Food Engineering*, *68*(3), 277–287, http://dx.doi.org/10.1016/j.jfoodeng.2004.05.044.

Dufour, É., Frencia, J. P., & Kane, E. (2003). Development of a rapid method based on front-face fluorescence spectroscopy for the monitoring of fish freshness. *Food Research International*, *36*(5), 415–423.

Elmasry, G., Kamruzzaman, M., Sun, D. -W., & Allen, P. (2012). Principles and applications of hyperspectral imaging in quality evaluation of agro-food products: A review. *Critical Reviews in Food Science and Nutrition*, *52*(11), 999–1023.

ElMasry, G., Sun, D. -W., & Allen, P. (2011). Non-destructive determination of water-holding capacity in fresh beef by using NIR hyperspectral imaging. *Food Research International*, *44*(9), 2624–2633.

ElMasry, G., Sun, D. -W., & Allen, P. (2012). Near-infrared hyperspectral imaging for predicting colour, pH and tenderness of fresh beef. *Journal of Food Engineering*, *110*(1), 127–140.

ElMasry, G., Sun, D. -W., & Allen, P. (2013). Chemical-free assessment and mapping of major constituents in beef using hyperspectral imaging. *Journal of Food Engineering*, *117*(2), 235–246.

Feng, Y. -Z., & Sun, D. -W. (2012). Application of hyperspectral imaging in food safety inspection and control: A review. *Critical Reviews in Food Science and Nutrition*, *52*(11), 1039–1058.

Feng, Y. -Z., & Sun, D. -W. (2013). Near-infrared hyperspectral imaging in tandem with partial least squares regression and genetic algorithm for non-destructive determination and visualization of *Pseudomonas* loads in chicken fillets. *Talanta*, *109*, 74–83.

Gallart-Jornet, L., Rustad, T., Barat, J., Fito, P., & Escriche, I. (2007). Effect of superchilled storage on the freshness and salting behaviour of Atlantic salmon (*Salmo salar*) fillets. *Food Chemistry*, *103*(4), 1268–1281.

Ghasemi-Varnamkhasti, M., Mohtasebi, S. S., Rodriguez-Mendez, M. L., Gomes, A. A., Araújo, M. C. U., & Galvão, R. K. (2012). Screening analysis of beer ageing using near infrared spectroscopy and the Successive Projections Algorithm for variable selection. *Talanta*, *89*, 286–291.

He, H. -J., Wu, D., & Sun, D. -W. (2013). Non-destructive and rapid analysis of moisture distribution in farmed Atlantic salmon (*Salmo salar*) fillets using visible and near-infrared hyperspectral imaging. *Innovative Food Science & Emerging Technologies*, *18*, 237–245.

Howard, D. L., & Kjaergaard, H. G. (2006). Influence of intramolecular hydrogen bond strength on OH-stretching overtones. *The Journal of Physical Chemistry. A*, *110*(34), 10245–10250.

Iglesias, J., Medina, I., Bianchi, F., Careri, M., Mangia, A., & Musci, M. (2009). Study of the volatile compounds useful for the characterisation of fresh and frozen–thawed cultured gilthead sea bream fish by solid-phase microextraction gas chromatography–mass spectrometry. *Food Chemistry*, *115*(4), 1473–1478.

Ivorra, E., Girón, J., Sánchez, A. J., Verdú, S., Barat, J. M., & Grau, R. (2013). Detection of expired vacuum-packed smoked salmon based on PLS-DA method using hyperspectral images. *Journal of Food Engineering*, *117*(3), 342–349.

Kamruzzaman, M., Barbin, D., ElMasry, G., Sun, D. -W., & Allen, P. (2012). Potential of hyperspectral imaging and pattern recognition for categorization and authentication of red meat. *Innovative Food Science & Emerging Technologies*, *16*, 312–325.

Kamruzzaman, M., ElMasry, G., Sun, D. -W., & Allen, P. (2012). Prediction of some quality attributes of lamb meat using near-infrared hyperspectral imaging and multivariate analysis. *Analytica Chimica Acta*, *714*, 57–67.

Karoui, R., Lefur, B., Grondin, C., Thomas, E., Demeulemester, C., Baerdemaeker, J.D., et al. (2007). Mid-infrared spectroscopy as a new tool for the evaluation of fish freshness. *International Journal of Food Science & Technology*, *42*(1), 57–64.

Kimiya, T., Sivertsen, A. H., & Heia, K. (2013). VIS/NIR spectroscopy for non-destructive freshness assessment of Atlantic salmon (*Salmo salar* L.) fillets. *Journal of Food Engineering*, *116*(3), 758–764.

Maleki, M., Mouazen, A., Ramon, H., & De Baerdemaeker, J. (2007). Multiplicative scatter correction during on-line measurement with near infrared spectroscopy. *Biosystems Engineering*, *96*(3), 427–433.

Mathiassen, J. R., Misimi, E., Bondø, M., Veliyulin, E., & Østvik, S. O. (2011). Trends in application of imaging technologies to inspection of fish and fish products. *Trends in Food Science & Technology*, *22*(6), 257–275.

Mendes, R., Cardoso, C., & Pestana, C. (2009). Measurement of malondialdehyde in fish: a comparison study between HPLC methods and the traditional spectrophotometric test. *Food Chemistry*, *112*(4), 1038–1045.

Menesatti, P., Costa, C., & Aguzzi, J. (2010). Quality evaluation of fish by hyperspectral imaging. *Hyperspectral imaging for food quality analysis and control*, *273–294*.

Misimi, E., Mathiassen, J., & Erikson, U. (2007). Computer vision-based sorting of Atlantic salmon (*Salmo salar*) fillets according to their color level. *Journal of Food Science*, *72*(1), S030–S035.

Moreira, E. D. T., Pontes, M. J. C., Galvão, R. K. H., & Araújo, M. C. U. (2009). Near infrared reflectance spectrometry classification of cigarettes using the successive projections algorithm for variable selection. *Talanta*, *79*(5), 1260–1264.

Nicolaï, B.M., Theron, K. I., & Lammertyn, J. (2007). Kernel PLS regression on wavelet transformed NIR spectra for prediction of sugar content of apple. *Chemometrics and Intelligent Laboratory Systems*, *85*(2), 243–252.

Nilsen, H., & Esaiassen, M. (2005). Predicting sensory score of cod (*Gadus morhua*) from visible spectroscopy. *LWT—Food Science and Technology*, *38*(1), 95–99.

Nilsen, H., Esaiassen, M., Heia, K., & Sigernes, F. (2002). Visible/near-infrared spectroscopy: A new tool for the evaluation of fish freshness? *Journal of Food Science*, *67*(5), 1821–1826.

Norton, T., & Sun, D. -W. (2008). Recent advances in the use of high pressure as an effective processing technique in the food industry. *Food and Bioprocess Technology*, *1*(1), 2–34.

Özogul, Y., Özyurt, G., Özogul, F., Kuley, E., & Polat, A. (2005). Freshness assessment of European eel (*Anguilla anguilla*) by sensory, chemical and microbiological methods. *Food Chemistry*, *92*(4), 745–751.

Park, B., Lawrence, K. C., Windham, W. R., & Smith, D. P. (2006). Performance of hyperspectral imaging system for poultry surface fecal contaminant detection. *Journal of Food Engineering*, *75*(3), 340–348.

Poli, B., Parisi, G., Scappini, F., & Zampacavallo, G. (2005). Fish welfare and quality as affected by pre-slaughter and slaughter management. *Aquaculture International*, *13*(1–2), 29–49.

Pons-Sanchez-Cascado, S., Vidal-Carou, M., Nunes, M., & Veciana-Nogues, M. (2006). Sensory analysis to assess the freshness of Mediterranean anchovies (*Engraulis encrasicholus*) stored in ice. *Food Control*, *17*(7), 564–569.

Pontes, M. J. C., Galvão, R. K. H., Araújo, M. C. U., Moreira, P. N. T., Neto, O. D. P., José, G. E., et al. (2005). The successive projections algorithm for spectral variable selection in classification problems. *Chemometrics and Intelligent Laboratory Systems*, *78*(1), 11–18.

Quevedo, R., & Aguilera, J. (2010). Computer vision and stereoscopy for estimating firmness in the salmon (*Salmon salar*) fillets. *Food and Bioprocess Technology*, *3*(4), 561–567.

Quevedo, R. A., Aguilera, J. M., & Pedreschi, F. (2010). Color of salmon fillets by computer vision and sensory panel. *Food and Bioprocess Technology*, *3*(5), 637–643.

Rinnan, Å., Berg, F. v. d., & Engelsen, S. B. (2009). Review of the most common pre-processing techniques for near-infrared spectra. *TrAC Trends in Analytical Chemistry*, *28*(10), 1201–1222.

Rzepka, M., Özogul, F., Surówka, K., & Michalczyk, M. (2013). Freshness and quality attributes of cold stored Atlantic bonito (*Sarda sarda*) gravad. *International Journal of Food Science & Technology*, *48*(6), 1318–1326.

Sivertsen, A. H., Heia, K., Hindberg, K., & Godtliebsen, F. (2012). Automatic nematode detection in cod fillets (*Gadus morhua* L.) by hyperspectral imaging. *Journal of Food Engineering*, *111*(4), 675–681.

Sivertsen, A. H., Heia, K., Stormo, S. K., Elvevoll, E., & Nilsen, H. (2011). Automatic nematode detection in cod fillets (*Gadus morhua*) by transillumination hyperspectral imaging. *Journal of Food Science*, *76*(1), S77–S83.

Sone, I., Olsen, R. L., Sivertsen, A. H., Eilertsen, G., & Heia, K. (2012). Classification of fresh Atlantic salmon (*Salmo salar* L.) fillets stored under different atmospheres by hyperspectral imaging. *Journal of Food Engineering*, *109*(3), 482–489.

Song, Y., Luo, Y., You, J., Shen, H., & Hu, S. (2011). Biochemical, sensory and microbiological attributes of bream (*Megalobrama amblycephala*) during partial freezing and chilled storage. *Journal of the Science of Food and Agriculture*, *92*(1), 197–202.

Sun, D. -W., & Brosnan, T. (1999, Sep). Extension of the vase life of cut daffodil flowers by rapid vacuum cooling. *International Journal of Refrigeration-Revue Internationale Du Froid*, *22*(6), 472–478, http://dx.doi.org/10.1016/S0140-7007(99)00011-0.

Sun, D. -W., & Hu, Z. H. (2003, Jan). CFD simulation of coupled heat and mass transfer through porous foods during vacuum cooling process. *International Journal of Refrigeration-Revue Internationale Du Froid*, *26*(1), 19–27, http://dx.doi.org/10.1016/S0140-7007(02)00038-5.

Sun, D. -W., & Zheng, L. Y. (2006, Nov). Vacuum cooling technology for the agri-food industry: Past, present and future. *Journal of food Engineering*, *77*(2), 203–214, http://dx.doi.org/10.1016/j.jfoodeng.2005.06.023.

Hyperspectral imaging for food quality analysis and control. Sun, Da-Wen (Ed.). (2010). San Diego, California, USA: Academic Press/Elsevier978-0-12-374753-2 (496 pp.).

Suykens, J. A., De Brabanter, J., Lukas, L., & Vandewalle, J. (2002). Weighted least squares support vector machines: Robustness and sparse approximation. *Neurocomputing*, *48*(1), 85–105.

Suykens, J. A., Vandewalle, J., & De Moor, B. (2001). Optimal control by least squares support vector machines. *Neural Networks*, *14*(1), 23–35.

Talens, P., Mora, L., Morsy, N., Barbin, D. F., ElMasry, G., & Sun, D. -W. (2013). Prediction of water and protein contents and quality classification of Spanish cooked ham using NIR hyperspectral imaging. *Journal of Food Engineering*, *117*(3), 272–280.

Tarr, A. W., & Zerbetto, F. (1989). Absolute intensities of CH-stretching overtones in chloroform and deuterochloroform. *Chemical Physics Letters*, *154*(3), 273–279.

Wang, L. J., & Sun, D. -W. (2001, May-Jun). *Rapid cooling of porous and moisture foods by using vacuum cooling technology. Trends in Food Science & Technology*, *12*(5–6), 174–184, http://dx.doi.org/10.1016/S0924-2244(01)00077-2.

Williams, P. J., Geladi, P., Britz, T. J., & Manley, M. (2012a). Growth characteristics of three *Fusarium* species evaluated by near-infrared hyperspectral imaging and multivariate image analysis. *Applied Microbiology and Biotechnology*, *96*(3), 803–813.

Williams, P. J., Geladi, P., Britz, T. J., & Manley, M. (2012b). Near-infrared (NIR) hyperspectral imaging and multivariate image analysis to study growth characteristics and differences between species and strains of members of the genus *Fusarium*. *Analytical and Bioanalytical Chemistry*, *404*(6–7), 1759–1769.

Wu, J., Peng, Y., Li, Y., Wang, W., Chen, J., & Dhakal, S. (2012). Prediction of beef quality attributes using VIS/NIR hyperspectral scattering imaging technique. *Journal of Food Engineering*, *109*(2), 267–273.

Wu, D., Shi, H., Wang, S., He, Y., Bao, Y., & Liu, K. (2012). Rapid prediction of moisture content of dehydrated prawns using online hyperspectral imaging system. *Analytica Chimica Acta*, *726*, 57–66.

Wu, D., & Sun, D. -W. (2013). Potential of time series-hyperspectral imaging (TS-HSI) for non-invasive determination of microbial spoilage of salmon flesh. *Talanta*, *111*, 39–46.

Wu, D., Sun, D. -W., & He, Y. (2012). Application of long-wave near infrared hyperspectral imaging for measurement of colour distribution in salmon fillet. *Innovative Food Science & Emerging Technologies*, *16*, 361–372.

Xiaobo, Z., Jiewen, Z., Povey, M. J., Holmes, M., & Hanpin, M. (2010). Variables selection methods in near-infrared spectroscopy. *Analytica Chimica Acta*, *667*(1), 14–32.

Xiccato, G., Trocino, A., Tulli, F., & Tibaldi, E. (2004). Prediction of chemical composition and origin identification of European sea bass (*Dicentrarchus labrax* L.) by near infrared reflectance spectroscopy (NIRS). *Food Chemistry*, *86*(2), 275–281.

Xu, S. Y., Chen, X. F., & Sun, D. -W. (2001, Dec). Preservation of kiwifruit coated with an edible film at ambient temperature. *Journal of Food Engineering*, *50*(4), 211–216, http://dx.doi.org/10.1016/S0260-8774(01)00022-X.

Zeaiter, M., Roger, J. -M., & Bellon-Maurel, V. (2005). Robustness of models developed by multivariate calibration. *Part II: The influence of pre-processing methods. TrAC Trends in Analytical Chemistry*, *24*(5), 437–445.

Zhang, X., Liu, F., He, Y., & Li, X. (2012). Application of hyperspectral imaging and chemometric calibrations for variety discrimination of maize seeds. *Sensors*, *12*(12), 17234–17246.

Zhu, F., Zhang, D., He, Y., Liu, F., & Sun, D. -W. (2012). Application of visible and near infrared hyperspectral imaging to differentiate between fresh and frozen-thawed fish fillets. *Food and Bioprocess Technology*, *1–7*.

Zion, B. (2012). The use of computer vision technologies in aquaculture—A review. *Computers and Electronics in Agriculture*, *88*, 125–132.